American Journal of Engineering Research (AJER)
e-ISSN: 2320-0847 p-ISSN: 2320-0936
Volume-15, Issue-5, pp-12-25
www.ajer.org
Research Paper Open Access

Turing Pattern Dynamics of Reaction-Diffusion Systems on Graphs

Changjian Wu[1,*], Ying Xiong[1]

[1](Zhujiang College , South China Agricultural University, Guangzhou, 510900, China)
*Corresponding Author: Ch.J. Wu

ABSTRACT : *This paper investigates the pattern dynamics of a class of discrete reaction-diffusion systems defined on finite, connected, undirected graphs without loops or multiple edges. The system consists of coupled difference equations augmented with diffusion terms described by the graph Laplacian operator. Taking the competitive Lotka–Volterra system as a concrete reaction scheme, linear stability analysis and numerical simulations reveal the conditions for Turing instability on graphs and demonstrate how graph topology modulates the resulting spatial patterns.*

KEYWORDS: *graph theory; reaction-diffusion systems; pattern dynamics; Turing instability; The Competitive Lotka-Volterra Model.*

Date of Submission: 28-04-2026 Date of acceptance: 08-05-2026

I. INTRODUCTION

Pattern dynamics concerns the spontaneous formation and evolution of spatial structures in spatially extended systems. Since Turing's seminal work [1], reaction-diffusion equations have served as the canonical framework for understanding morphogenesis and self-organization phenomena. While classical studies predominantly focus on continuous Euclidean domains, many real-world systems possess inherently discrete, networked architectures—examples include neuronal networks, ecological food webs, and social interaction graphs.

Nakao and Mikhailov [2] first generalized reaction-diffusion processes to complex networks, establishing the theoretical foundation for Turing patterns on graphs. Subsequent developments have extended these ideas to coupled oscillator synchronization [3], epidemic spreading on networks [4], and biological pattern formation [5]. Building upon this foundation, this paper investigates the pattern dynamics of a class of discrete reaction-diffusion systems defined on finite, connected, undirected graphs without loops or multiple edges.

The remainder of the paper is organized as follows. Section 2 presents the mathematical model and theoretical framework. Section 3 introduces the competitive Lotka–Volterra system used for numerical studies. Section 4 reports extensive numerical experiments. We select an N×N regular grid graph with 4-neighbor connectivity, considering both periodic and Neumann boundary conditions. Numerical simulations are carried out

on these graphs, and a rich variety of patterns are obtained. Section 5 concludes with a discussion of the implications and future research directions.

II. Model and Theoretical Framework

2.1 Graph Structure and Basic Definitions

Let $G = (V, E)$ be a connected, finite, undirected graph without loops or multiple edges. The vertex set is $V = \{1, 2, \ldots, n\}$, and the edge set is

$$E = \{(i, j) \mid i \sim j,\ i \in V,\ j \in V\}, \tag{1}$$

where $i \sim j$ denotes that vertices i and j are adjacent.

Definition 1 *The graph Laplacian operator is defined as*

$$\Delta u(i) = \sum_{j \sim i} [u(i) - u(j)],\ i \in V, \tag{2}$$

where $u(i)$ are real-valued functions defined on the vertex set. In matrix form, $\mathbf{L} = \mathbf{D} - \mathbf{A}$, *where* $\mathbf{A}$ *is the adjacency matrix and* $\mathbf{D} = \mathrm{diag}(d_1, \ldots, d_n)$ *is the degree matrix with* $d_i = \sum_{j=1}^{n} A_{ij}$.

For more details on graphs and Laplacian matrices, please refer to [6].

2.2 Reaction-Diffusion System

On the graph G, we consider the following discrete dynamical system without diffusion:

$$\begin{cases} u_{t+1}(i) = f[u_t(i), v_t(i)], \\ v_{t+1}(i) = g[u_t(i), v_t(i)], \end{cases} \quad i \in V,\ t \in \square^{+}, \tag{3}$$

where $u(i), v(i)$ are real-valued functions defined on the vertex set, and $f(u,v), g(u,v)$ are assumed to be sufficiently smooth.

Assumption 1 (Existence of Uniform Fixed Point) *System* (3) *admits a spatially uniform fixed point* (u^*, v^*) *satisfying*

$$u^* = f(u^*, v^*),\quad v^* = g(u^*, v^*).' \tag{4}$$

Upon introducing diffusion terms, we obtain the reaction-diffusion system on the graph:

$$\begin{cases} u_{t+1}(i) = f[u_t(i), v_t(i)] - d_1 \Delta u_t(i), \\ v_{t+1}(i) = g[u_t(i), v_t(i)] - d_2 \Delta v_t(i), \end{cases} \quad i \in V,\ t \in \square^{+}, \tag{5}$$

where $d_1, d_2 \geq 0$ are diffusion coefficients. Evidently, the uniform fixed point (u^*, v^*) of system (3) remains a fixed point of system (5).

2.3 Linear Stability and Turing Conditions

Let

$$\mathbf{u} = (u(1), u(2), \ldots, u(n))^T,\ \mathbf{v} = (v(1), v(2), \ldots, v(n))^T, , \tag{6}$$

and the small perturbation of $\mathbf{u}, \mathbf{v}$ at the fixed point (u^*, v^*) are given by

$$\delta\mathbf{u} = \mathbf{u} - u^*\mathbf{e},\ \delta\mathbf{v} = \mathbf{v} - u^*\mathbf{e}, , \tag{7}$$

Where $\mathbf{e} = (1, 1, \ldots, 1)^T$.

Linearizing system (5) about the uniform steady state (u^*, v^*) yields

$$\begin{pmatrix}\delta\mathbf{u}_{t+1}\\ \delta\mathbf{v}_{t+1}\end{pmatrix}=\begin{pmatrix}f_u\mathbf{I}-d_1\mathbf{L} & f_v\mathbf{I}\\ g_u\mathbf{I} & g_v\mathbf{I}-d_2\mathbf{L}\end{pmatrix}\begin{pmatrix}\delta\mathbf{u}_t\\ \delta\mathbf{v}_t\end{pmatrix}, \tag{8}$$

where the partial derivatives $f_u=\partial f/\partial u, f_v=\partial f/\partial v$, $g_u=\partial g/\partial u, g_v=\partial g/\partial v$ are evaluated at (u^*,v^*), and $\mathbf{I}$ denotes the $n\times n$ identity matrix.

Let $\mathbf{L}\varphi_\alpha=\lambda_\alpha\varphi_\alpha\ (\alpha=0,1,...,n-1)$ be the eigendecomposition of the graph Laplacian, and $\varphi_\alpha(\alpha=0,1,\cdots,n-1)$ is a set of standard orthonormal basis in R^n. The eigenvalues are ordered as $0=\lambda_0\le\lambda_1\le\cdots\le\lambda_{n-1}$, where $\lambda_0=0$ corresponds to the uniform eigenvector $\phi_0=(1,1,\ldots,1)^T/\sqrt{n}$.

Theorem 2 (Mode Decomposition) *By expanding perturbations in the Laplacian eigenbasis, each mode decouples and evolves according to*

$$\begin{pmatrix}\delta u_{t+1}^\alpha\\ \delta v_{t+1}^\alpha\end{pmatrix}=\begin{pmatrix}f_u-d_1\lambda_\alpha & f_v\\ g_u & g_v-d_2\lambda_\alpha\end{pmatrix}\begin{pmatrix}\delta u_t^\alpha\\ \delta v_t^\alpha\end{pmatrix}, \tag{9}$$

The corresponding characteristic equation is

$$P_\alpha(\sigma)=\sigma^2-\tau_\alpha\sigma+\Delta_\alpha=0,\quad(\alpha=0,1,\cdots,n-1), \tag{10}$$

where

$$\tau_\alpha=f_u+g_v-(d_1+d_2)\lambda_\alpha,\ \Delta_\alpha=(f_u-d_1\lambda_\alpha)(g_v-d_2\lambda_\alpha)-f_vg_u\ . \tag{11}$$

Proof. Decompose $\delta\mathbf{u}_{t+1}$, $\delta\mathbf{v}_{t+1}$, $\delta\mathbf{u}_t$, $\delta\mathbf{v}_t$ in R^n as

$$\delta\mathbf{u}_{t+1}=\sum_{\alpha=0}^{n-1}\delta u_{t+1}^\alpha\phi_\alpha,\ \delta\mathbf{v}_{t+1}=\sum_{\alpha=0}^{n-1}\delta v_{t+1}^\alpha\phi_\alpha,\ \delta\mathbf{u}_t=\sum_{\alpha=0}^{n-1}\delta u_t^\alpha\phi_\alpha,\ \delta\mathbf{v}_t=\sum_{\alpha=0}^{n-1}\delta v_t^\alpha\phi_\alpha\ .$$

then equation (8) can be transformed into

$$\sum_{\alpha=0}^{n-1}\begin{pmatrix}\delta u_{t+1}^\alpha\phi_\alpha\\ \delta v_{t+1}^\alpha\phi_\alpha\end{pmatrix}=\begin{pmatrix}f_u\mathbf{I}-d_1\mathbf{L} & f_v\mathbf{I}\\ g_u\mathbf{I} & g_v\mathbf{I}-d_2\mathbf{L}\end{pmatrix}\sum_{\alpha=0}^{n-1}\begin{pmatrix}\delta u_t^\alpha\phi_\alpha\\ \delta v_t^\alpha\phi_\alpha\end{pmatrix}.$$

Since $\varphi_\alpha(\alpha=0,1,\cdots,n-1)$ is a set of standard orthonormal basis in R^n , multiplying both sides of the above equation on the left by

$$\begin{pmatrix}\phi_\alpha^T & 0\\ 0 & \phi_\alpha^T\end{pmatrix},\quad(\alpha=0,1,\cdots,n-1),$$

yields

$$\begin{pmatrix}\delta u_{t+1}^\alpha\\ \delta v_{t+1}^\alpha\end{pmatrix}=\begin{pmatrix}f_u-d_1\lambda_\alpha & f_v\\ g_u & g_v-d_2\lambda_\alpha\end{pmatrix}\begin{pmatrix}\delta u_t^\alpha\\ \delta v_t^\alpha\end{pmatrix},\quad(\alpha=0,1,\cdots,n-1).$$

The corresponding characteristic equation is

$$\begin{vmatrix}\sigma-(f_u-d_1\lambda_\alpha) & -f_v\\ -g_u & \sigma-(g_v-d_2\lambda_\alpha)\end{vmatrix}=0,\quad(\alpha=0,1,\cdots,n-1),$$

namely

$$P_\alpha(\sigma)=\sigma^2-\tau_\alpha\sigma+\Delta_\alpha=0,\quad(\alpha=0,1,\cdots,n-1),$$

where $\tau_\alpha = f_u + g_v - (d_1 + d_2)\lambda_\alpha$, $\Delta_\alpha = (f_u - d_1\lambda_\alpha)(g_v - d_2\lambda_\alpha) - f_v g_u$. ■

Definition 3 (Turing Instability) *For given $d_1 > 0$, $d_2 > 0$, the uniform fixed point(u^*, v^*) is said to be Turing unstable if:*

(i) It is locally asymptotically stable in the absence of diffusion, i.e., $|\sigma(0)| < 1$;

(ii) There exists at least one mode $\lambda_\alpha > 0$ for which $|\sigma(\lambda_\alpha)| > 1$.

III. THE COMPETITIVE LOTKA-VOLTERRA MODEL

We adopt the competitive Lotka-Volterra system:

$$\begin{cases} u_{t+1}(i) = r_1 u_t(i)(1 - u_t(i) - a_1 v_t(i)), \\ v_{t+1}(i) = r_2 v_t(i)(1 - a_2 u_t(i) - v_t(i)), \end{cases} \quad i \in V,\ t \in \mathbb{Z}^+, \tag{12}$$

where $r_1 > 1, r_2 > 1, a_1 > 0$ and $a_2 > 0$, see [7].

Let

$$f(u,v) = r_1 u(1 - u - a_1 v),\ g(u,v) = r_2 v(1 - a_2 u - v). \tag{13}$$

Proposition 4 (Uniform Fixed Point) *For the parameter values $r_1 = r_2 = 2$, $a_1 = a_2 = 0.5$, system* (12) *admits a unique positive uniform fixed point given by*

$$(u^*, v^*) = \left(\frac{1}{3}, \frac{1}{3}\right). \tag{14}$$

Proof. The fixed point equations are

$$\begin{cases} 2u^*(1 - u^* - 0.5v^*) = u^*, \\ 2v^*(1 - 0.5u^* - v^*) = v^*. \end{cases}$$

By calculation, it is easy to obtain $u^* = v^* = \frac{1}{3}$. ■

Next, let $r_1 = r_2 = 2$, $a_1 = a_2 = 0.5$. We will discuss the Turing instability of system(12) at the fixed point $\left(\frac{1}{3}, \frac{1}{3}\right)$.

Upon introducing diffusion terms, we obtain the reaction-diffusion system on the graph:

$$\begin{cases} u_{t+1}(i) = 2u_t(i)(1 - u_t(i) - 0.5v_t(i)) - d_1 \Delta u_t(i), \\ v_{t+1}(i) = 2v_t(i)(1 - 0.5u_t(i) - v_t(i)) - d_2 \Delta v_t(i), \end{cases} \quad i \in V,\ t \in \mathbb{Z}^+, \tag{15}$$

and

$$f(u,v) = 2u(1 - u - 0.5v),\ g(u,v) = 2v(1 - 0.5u - v). \tag{16}$$

By calculation, it is easy to obtain

$$f_u\left(\frac{1}{3}, \frac{1}{3}\right) = \frac{1}{3},\ f_v\left(\frac{1}{3}, \frac{1}{3}\right) = -\frac{1}{3},\ g_u\left(\frac{1}{3}, \frac{1}{3}\right) = -\frac{1}{3},\ g_v\left(\frac{1}{3}, \frac{1}{3}\right) = \frac{1}{3}. \tag{17}$$

According to Theorem 2, the corresponding characteristic equation of (15) is

$$P_\alpha(\sigma) = \sigma^2 - \tau_\alpha \sigma + \Delta_\alpha = 0,\ \ (\alpha = 0, 1, \cdots, n-1), \tag{18}$$

where

$$\tau_\alpha = \frac{2}{3} - (d_1 + d_2)\lambda_\alpha, \quad \Delta_\alpha = d_1 d_2 \lambda_\alpha^2 - \frac{1}{3}(d_1 + d_2)\lambda_\alpha \ . \tag{19}$$

Proposition 5 (Roots of The Characteristic Equation) *Let* $d_1 = d_2 = d$, *then the roots of the characteristic equation* (18) *are* $\sigma_1(\lambda_\alpha) = -d\lambda_\alpha$ *and* $\sigma_2(\lambda_\alpha) = \frac{2}{3} - d\lambda_\alpha$.

Proof. When $d_1 = d_2 = d$, the corresponding characteristic equation of (18) is

$$P_\alpha(\sigma) = \sigma^2 - 2\left(\frac{1}{3} - d\lambda_\alpha\right)\sigma + d^2\lambda_\alpha^2 - \frac{2}{3}d\lambda_\alpha = 0, \quad (\alpha = 0,1,\cdots,n-1).$$

By calculation, it is easy to obtain its roots as $\sigma_1(\lambda_\alpha) = -d\lambda_\alpha$ *and* $\sigma_2(\lambda_\alpha) = \frac{2}{3} - d\lambda_\alpha$.

Theorem 6 *Assuming* $d_1 = d_2 = d$, *then when* $d > \frac{1}{\lambda_{n-1}}$, *the uniform fixed point* $\left(\frac{1}{3}, \frac{1}{3}\right)$ *of* (12) *is Turing unstable.*

Proof. According to Proposition 5, we have $\sigma_1(\lambda_\alpha) = -d\lambda_\alpha$ and $\sigma_2(\lambda_\alpha) = \frac{2}{3} - d\lambda_\alpha$. Obviously, $|\sigma_1(0)| = 0 < 1$ and $|\sigma_2(0)| = \frac{2}{3} < 1$ for $\lambda_0 = 0$. Namely, It is locally asymptotically stable in the absence of diffusion. When $d > \frac{1}{\lambda_{n-1}}$, we have

$$\sigma_1(\lambda_{n-1}) = -d\lambda_{n-1} < -\frac{1}{\lambda_{n-1}}\lambda_{n-1} = -1.$$

That is to say $|\sigma_1(\lambda_{n-1})| > 1$. Therefore, by Definition 3, the uniform fixed point $\left(\frac{1}{3}, \frac{1}{3}\right)$ of (12) is Turing unstable. ■

Remark: λ_{n-1} is the maximum eigenvalue of the Laplacian matrix **L**.

IV. NUMERICAL EXPERIMENTS

In this section, we perform numerical simulations of system (15) on different graphs to investigate the resulting Turing patterns. The graphs used are $N \times N$ 4-neighbor regular grid graphs, with boundary conditions taken as either 'periodic' or 'Neumann'. The initial condition is the uniform steady state (u∗,v∗) perturbed by additive Gaussian noise of amplitude 10^{-3} . Let $d_1 = d_2 = d$. And we take N=10 and N=100, respectively. By selecting appropriate values of d, we observe the Turing patterns of system (15) after 10,000, 100,000, and 200,000 iterations.

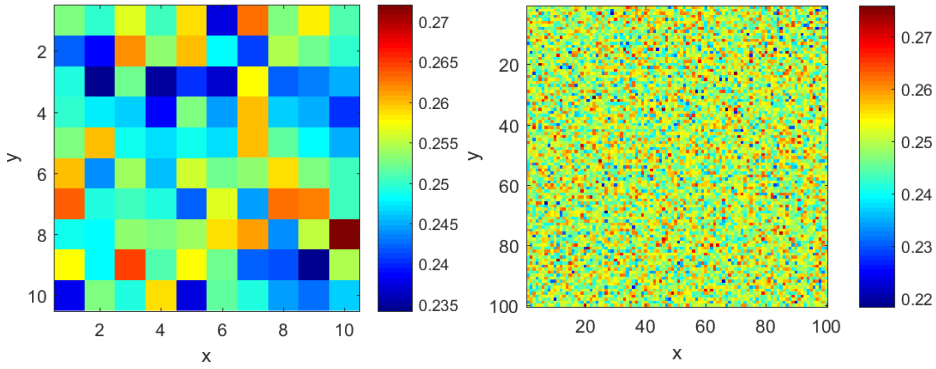

Fig.1. Initial condition plot (left: N=10, right:N=100)

4.1 The 4-Neighbor Regular Grid Graphs with Periodic Boundary Conditions

The eigenvalues of the Laplacian matrix for a $N \times N$ 4-neighbor regular grid graph with periodic boundary conditions are given by

$$\lambda_{ij} = 4 - 2\cos\left(\frac{2i\pi}{N}\right) - 2\cos\left(\frac{2j\pi}{N}\right), \ (i, j = 0,1,\cdots,N-1), \tag{19}$$

see [8]. When N is even, its maximum eigenvalue is 8; when N is odd, its maximum eigenvalue is very close to but less than 8. According to Theorem 6, when $d > \frac{1}{\lambda_{\max}}$, a Turing bifurcation occurs at the fixed point (14) of system (15).

It can be seen from Figures 2 and 3 that when d=0.1, system (15) converges to the fixed point $\left(\frac{1}{3}, \frac{1}{3}\right)$ for both N=10 and N=100.

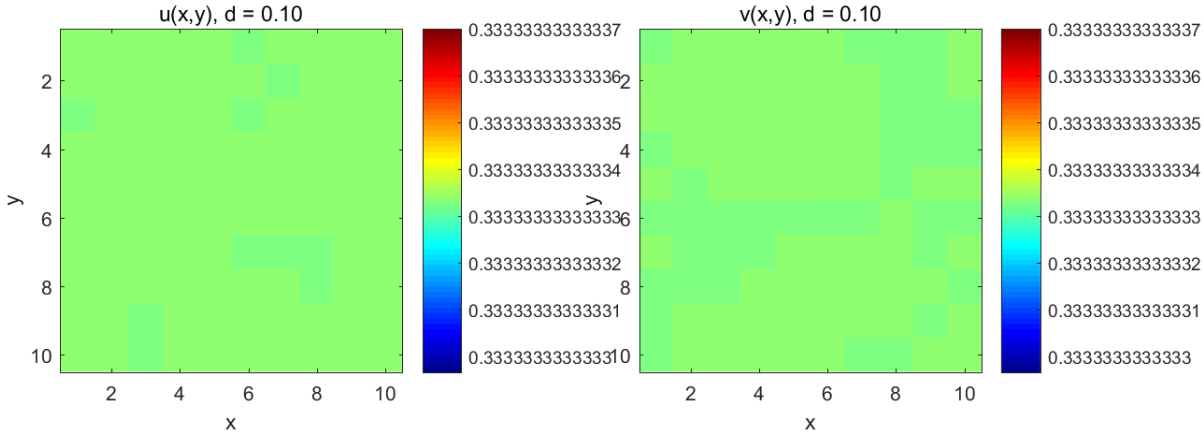

Fig.2. N=10, d=0.1, after 10,000 iterations (periodic boundary conditions)

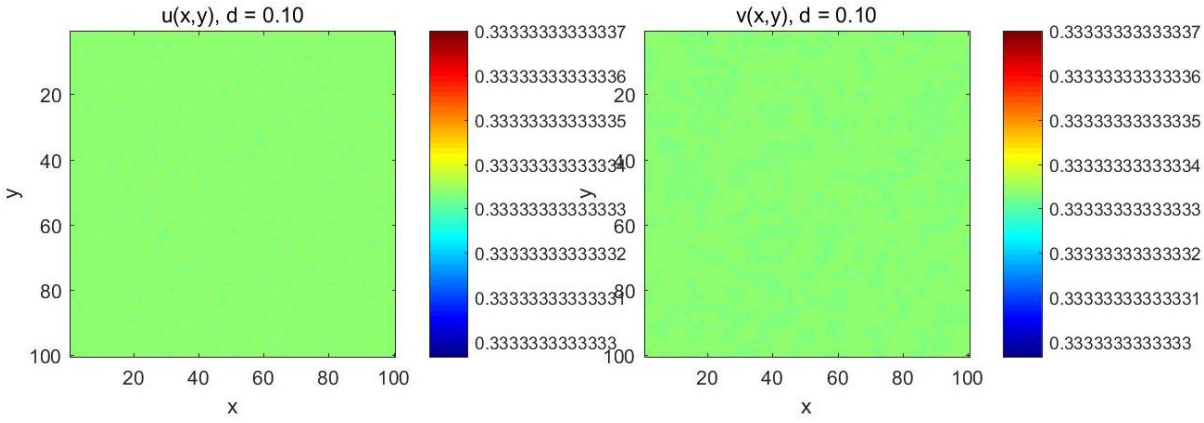

Fig.3. N=100, d=0.1, after 10,000 iterations (periodic boundary conditions)

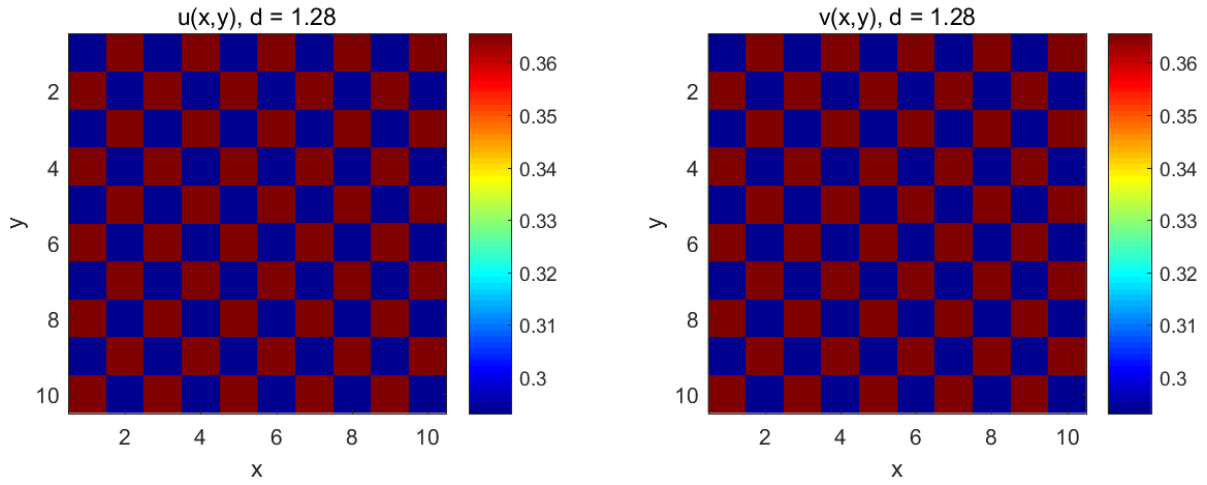

Fig.4. N=10, d=1.28, after 10,000 iterations (periodic boundary conditions)

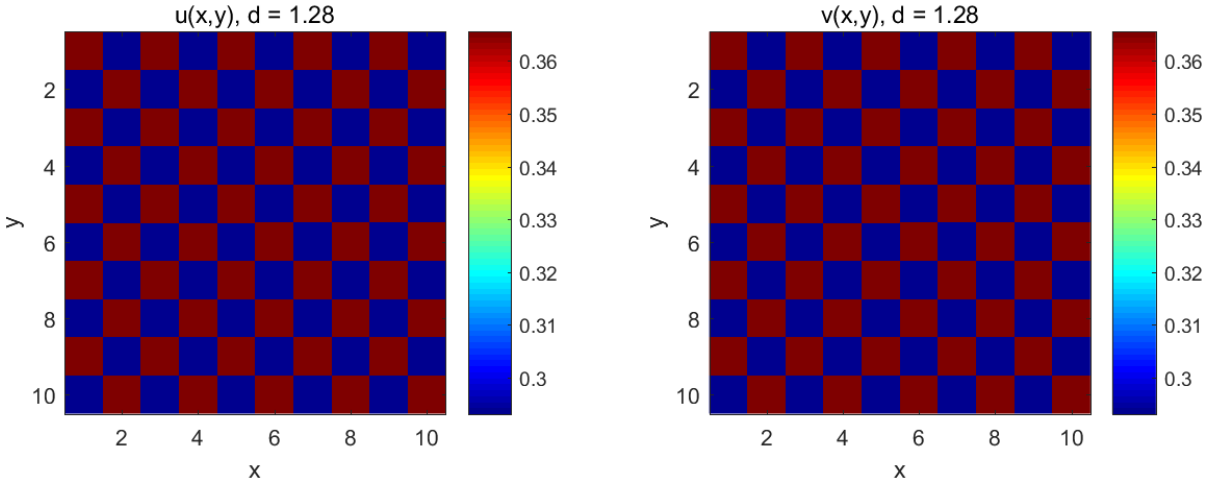

Fig.5. N=10, d=1.28, after 10,001 iterations (periodic boundary conditions)

It can be seen from Figures 4 and 5 that when d=1.28 and N=10, system (15) converges to a period-2 orbit.

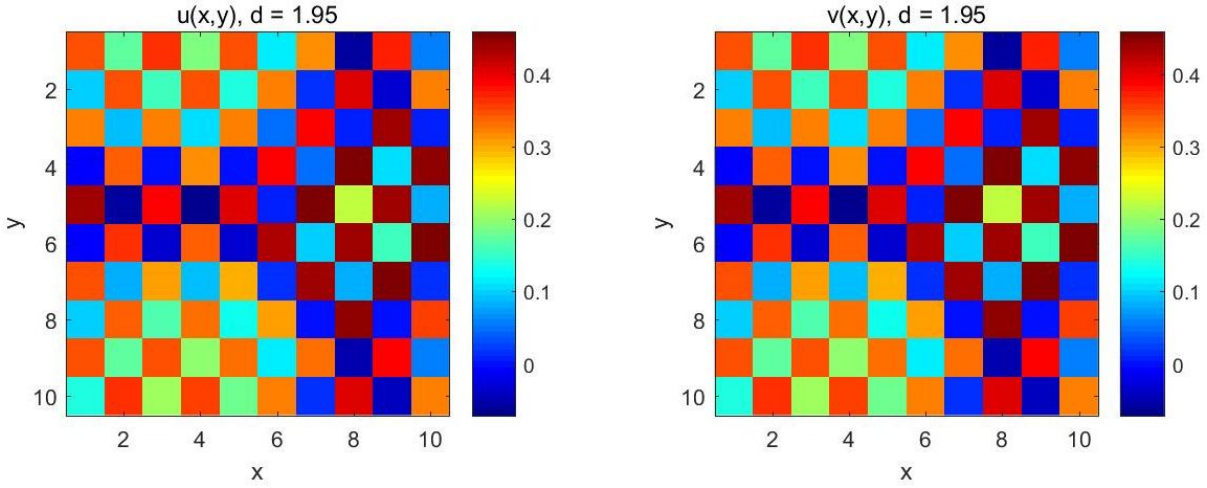

Fig.6. N=10, d=1.95, after 10,000 iterations (periodic boundary conditions)

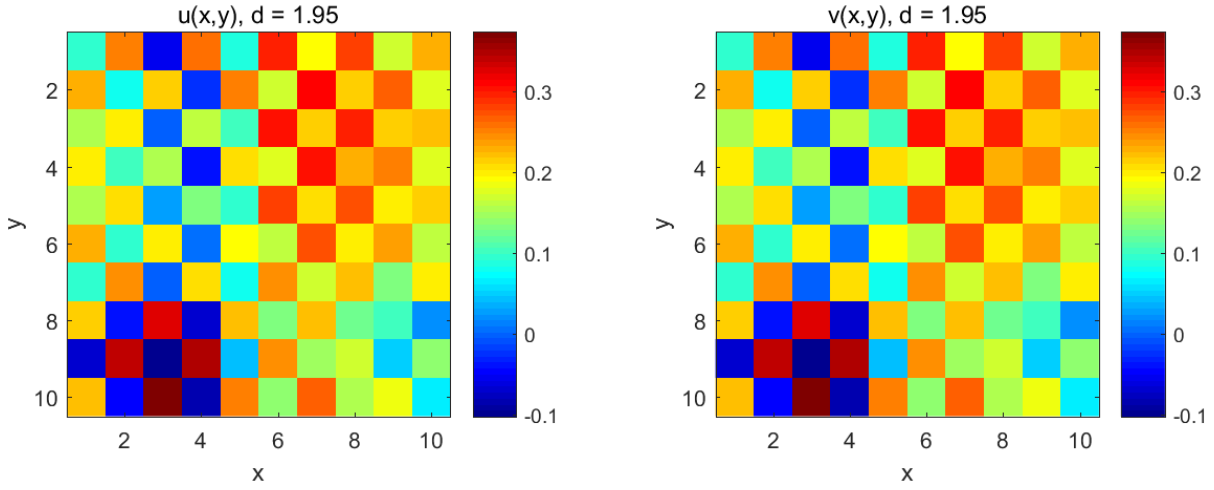

Fig.7. N=10, d=1.95, after 200,000 iterations (periodic boundary conditions)

It can be seen from Figures 6 and 7 that when d=1.95 and N=10, after 200,000 iterations, the values of u and v lie between -0.1 and 0.4, with no periodicity observed, indicating that the system has entered a chaotic state.

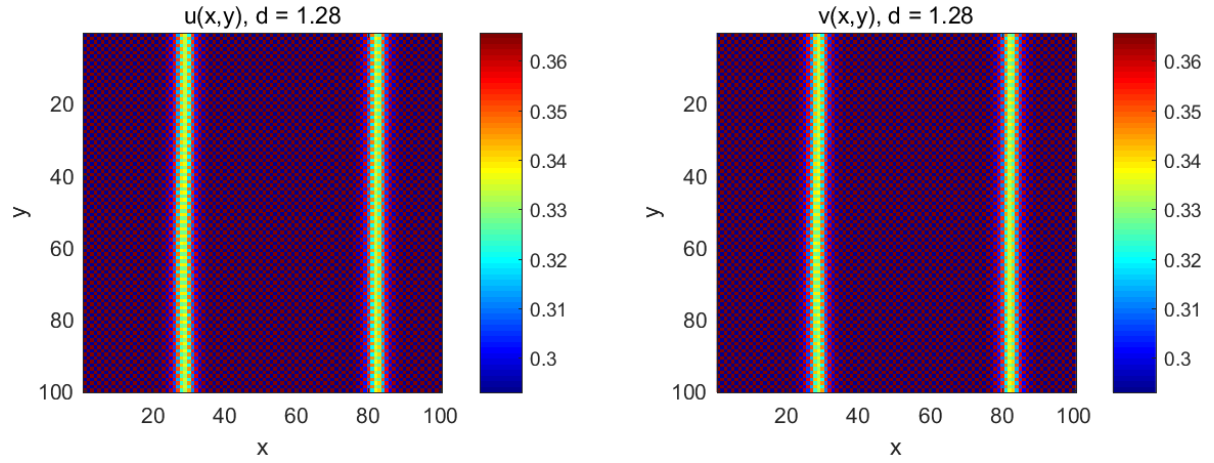

Fig.8. N=100, d=1.28, after 10,000 iterations (periodic boundary conditions)

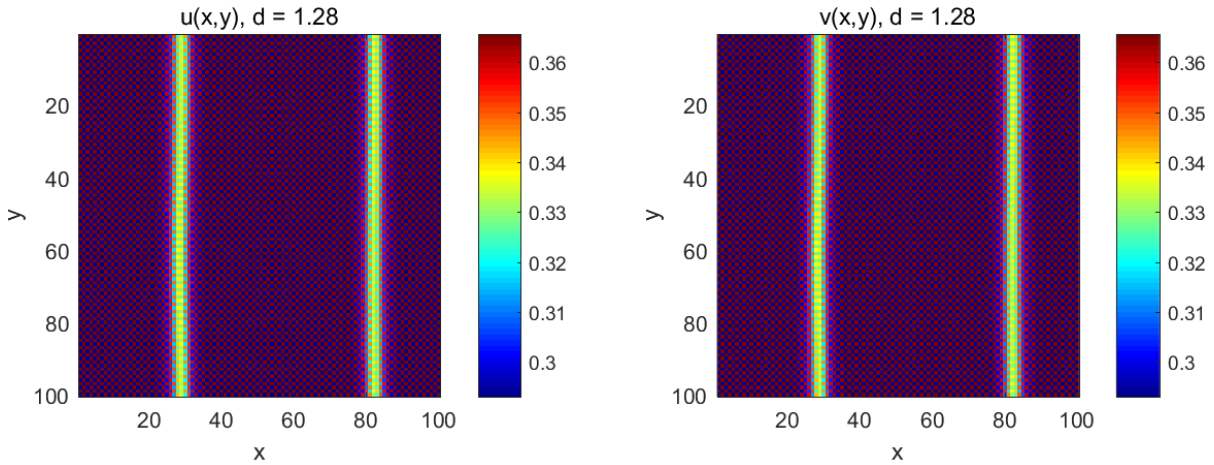

Fig.9. N=100, d=1.28, after 10,001 iterations (periodic boundary conditions)

It can be seen from Figures 4 and 5 that when d=1.28 and N=100, after 10,000 iterations, system (15)

converges to a period-2 orbit, and two distinct parallel line segments appear in the pattern.

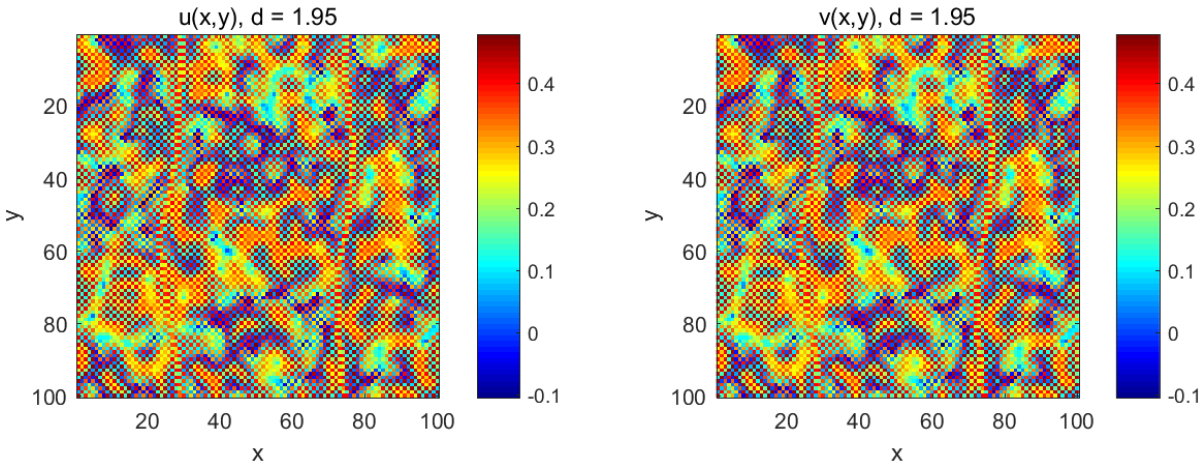

Fig.10. N=100, d=1.95, after 10,000 iterations (periodic boundary conditions)

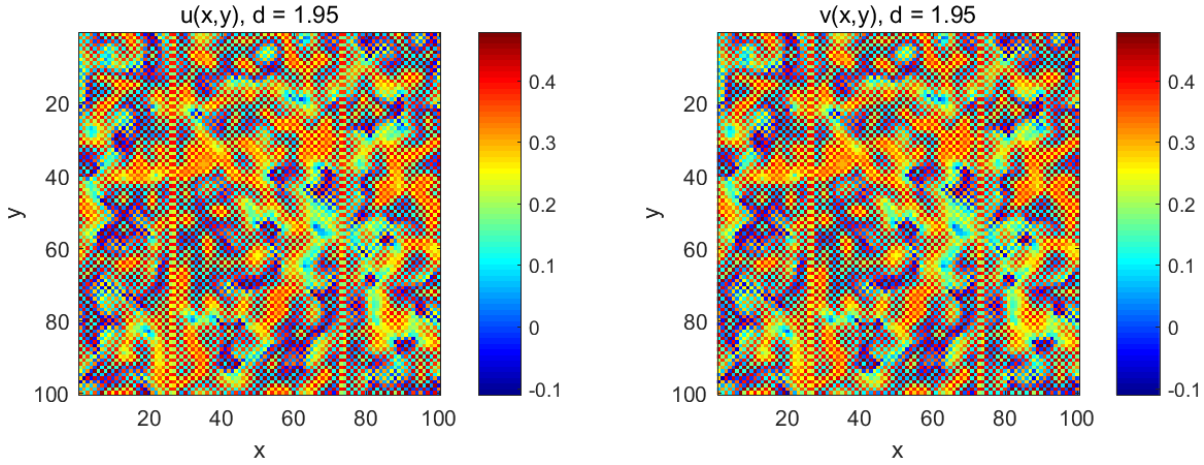

Fig.11. N=100, d=1.95, after 100,000 iterations (periodic boundary conditions)

It can be seen from Figures 10 and 11 that when d=1.95 and N=100, the values of u and v lie between −0.1 and 0.4. The patterns exhibit rich colors, and after 100,000 iterations, two distinct parallel line segments can be observed.

4.2 The 4-Neighbor Regular Grid Graphs with Neumann Boundary Conditions

The eigenvalues of the Laplacian matrix for a $N \times N$ 4-neighbor regular grid graph with Neumann boundary conditions are given by

$$\lambda_{ij} = 4 - 2\cos\left(\frac{i\pi}{N}\right) - 2\cos\left(\frac{j\pi}{N}\right), \ (i, j = 0,1,\cdots,N-1), \tag{20}$$

see [8]. Its maximum eigenvalue is very close to but less than 8.

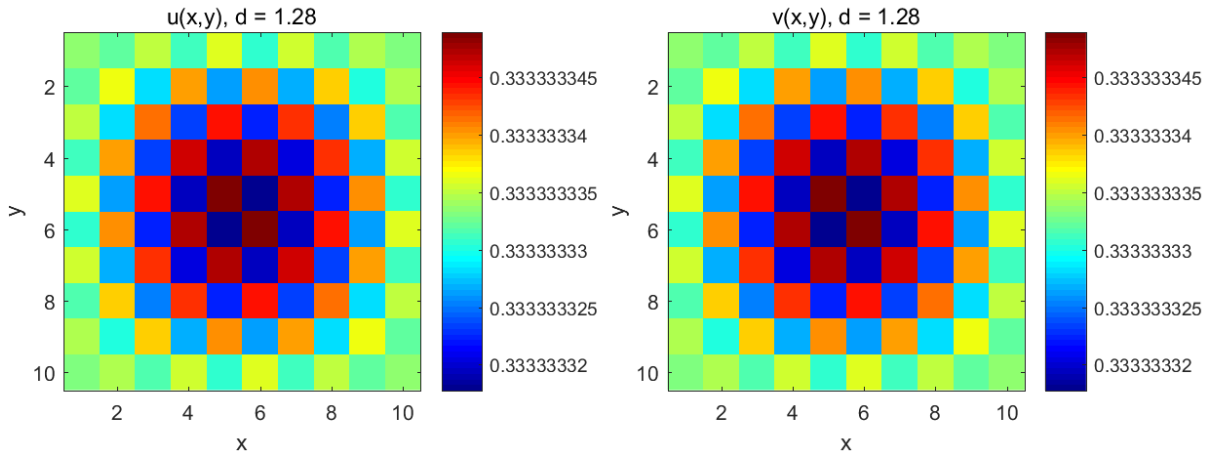

Fig.12. N=10, d=1.28, after 10,000 iterations (Neumann boundary conditions)

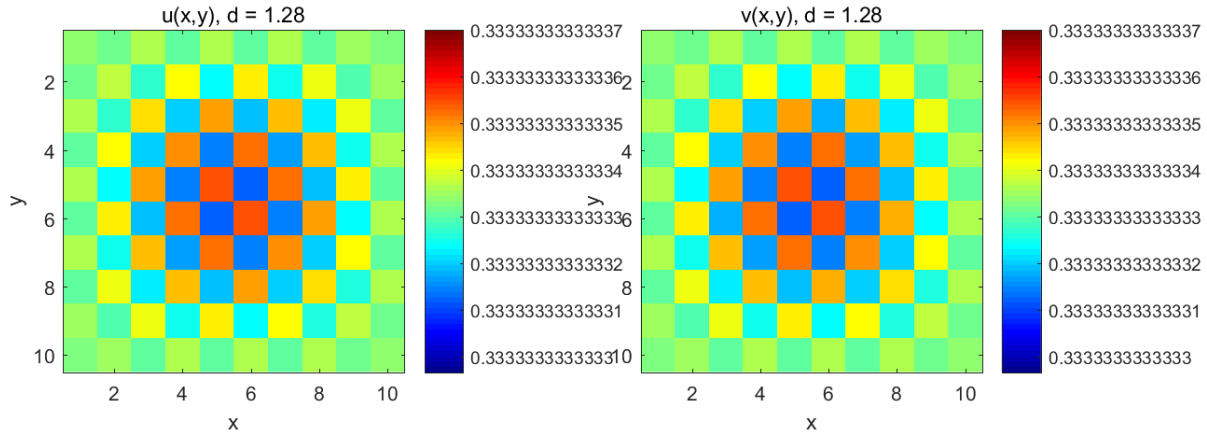

Fig.13. N=10, d=1.28, after 200,000 iterations (Neumann boundary conditions)

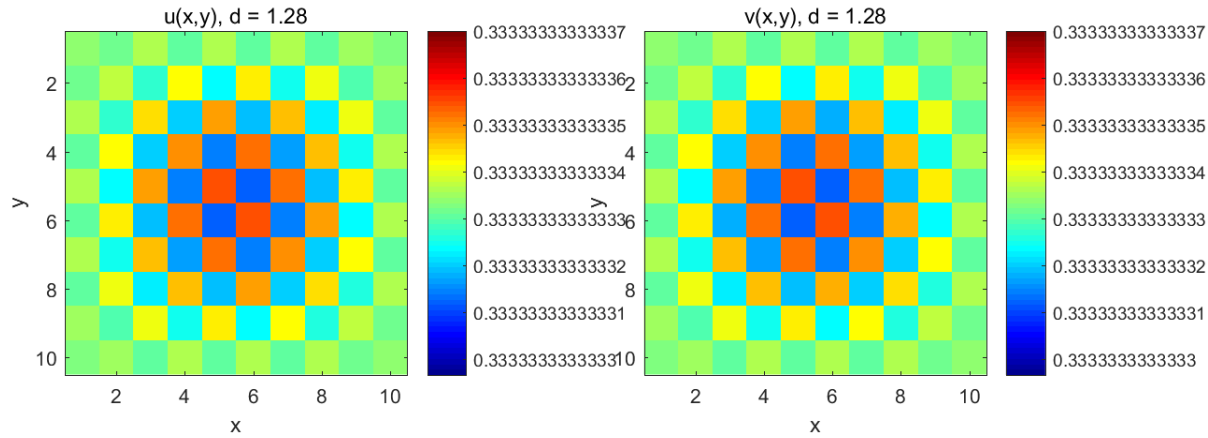

Fig.14. N=10, d=1.28, after 500,000 iterations (Neumann boundary conditions)

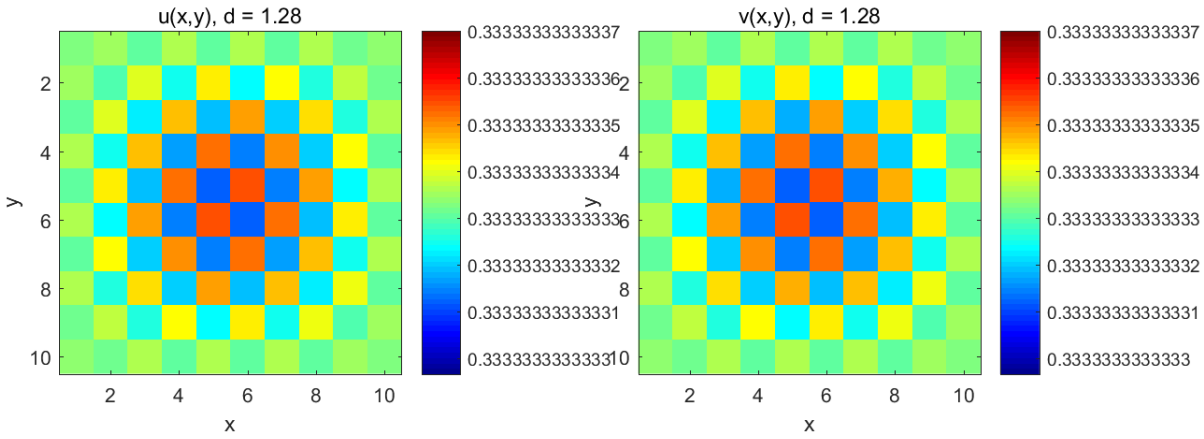

Fig.15. N=10, d=1.28, after 500,001 iterations (Neumann boundary conditions)

It can be seen from Figures 12 to 15 that when d=1.28 and N=10, the values of u and v remain near the fixed point. The pattern after 200,000 iterations is the same as that after 500,000 iterations, but differs from the pattern after 500,001 iterations. This indicates that the system has likely entered a periodic orbit.

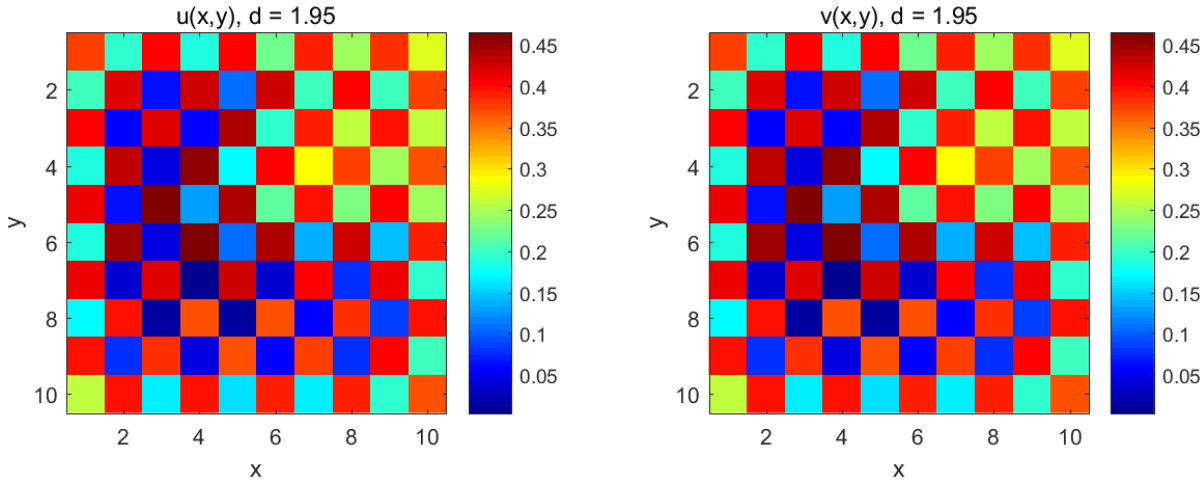

Fig.16. N=10, d=1.95, after 10,000 iterations (Neumann boundary conditions)

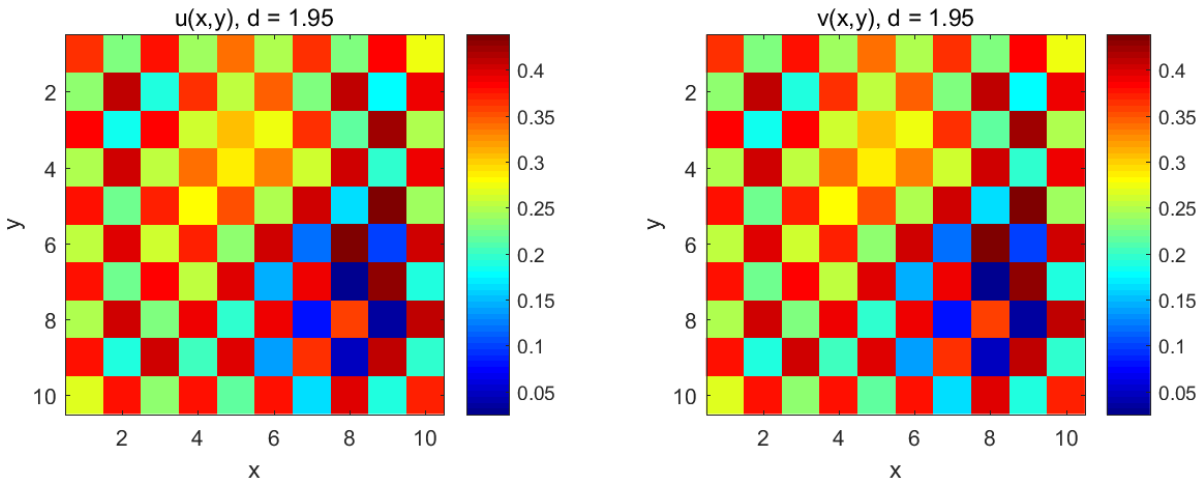

Fig.17. N=10, d=1.95, after 200,000 iterations (Neumann boundary conditions)

It can be seen from Figures 16 and 17 that when d=1.95 and N=10, after 200,000 iterations, the values of u and v lie between 0 and 0.45, with no periodicity observed, indicating that the system has entered a chaotic

state.

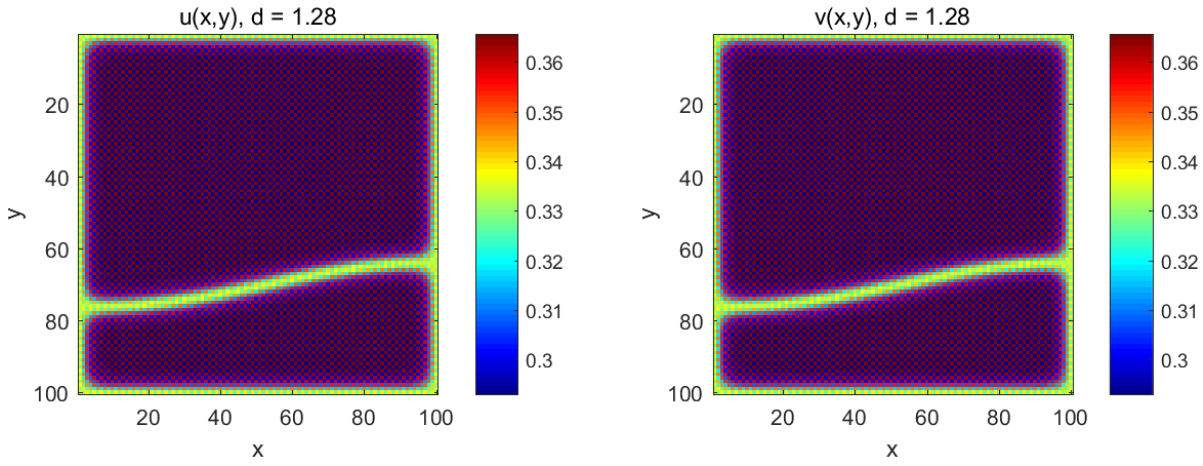

Fig.18. N=100, d=1.28, after 10,000 iterations (Neumann boundary conditions)

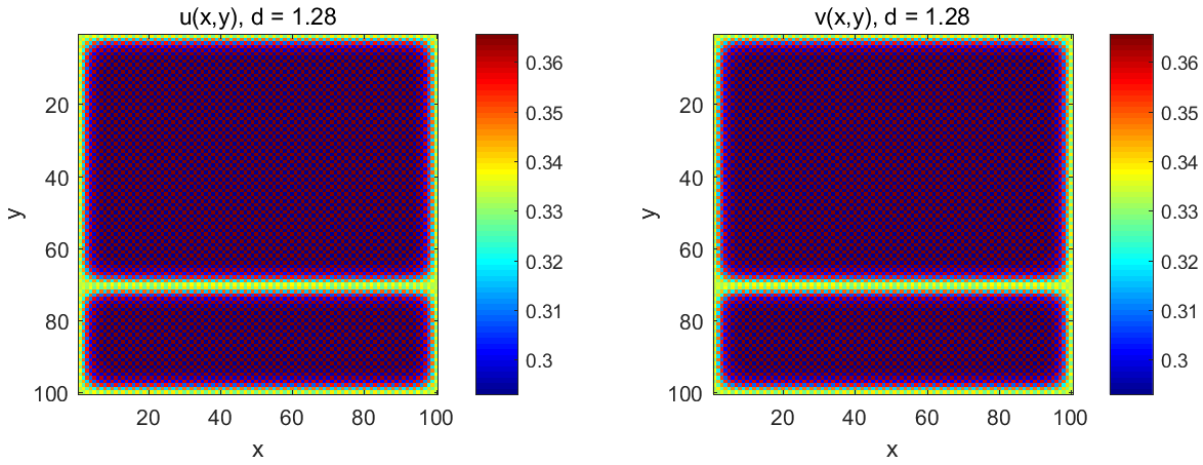

Fig.19. N=100, d=1.28, after 200,000 iterations (Neumann boundary conditions)

When d=1.28 and N=100, a curve appears in the pattern after 10,000 iterations, and after 200,000 iterations, this curve becomes a straight line segment. From the figures, it can be observed that the system has likely entered a periodic orbit.

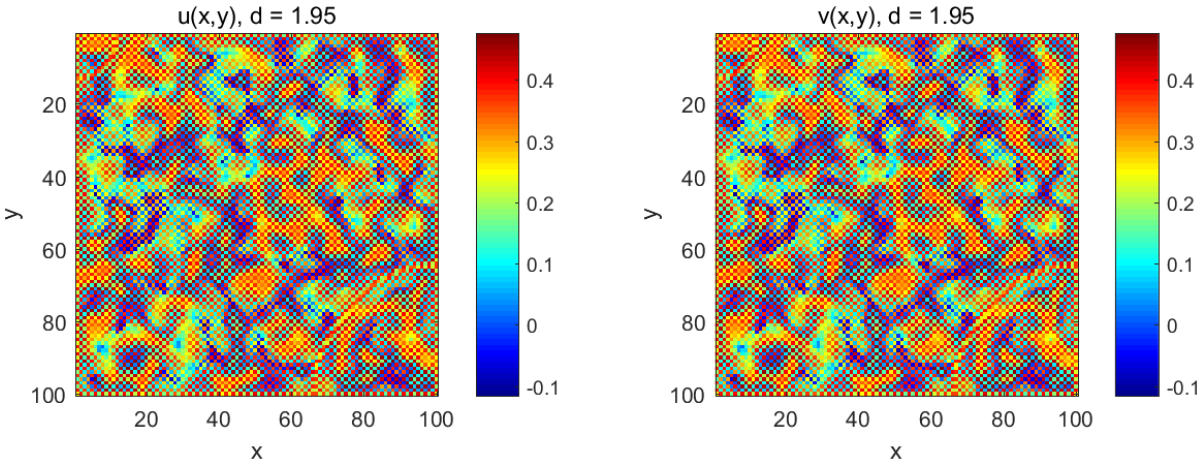

Fig.20. N=100, d=1.95, after 10,000 iterations (Neumann boundary conditions)

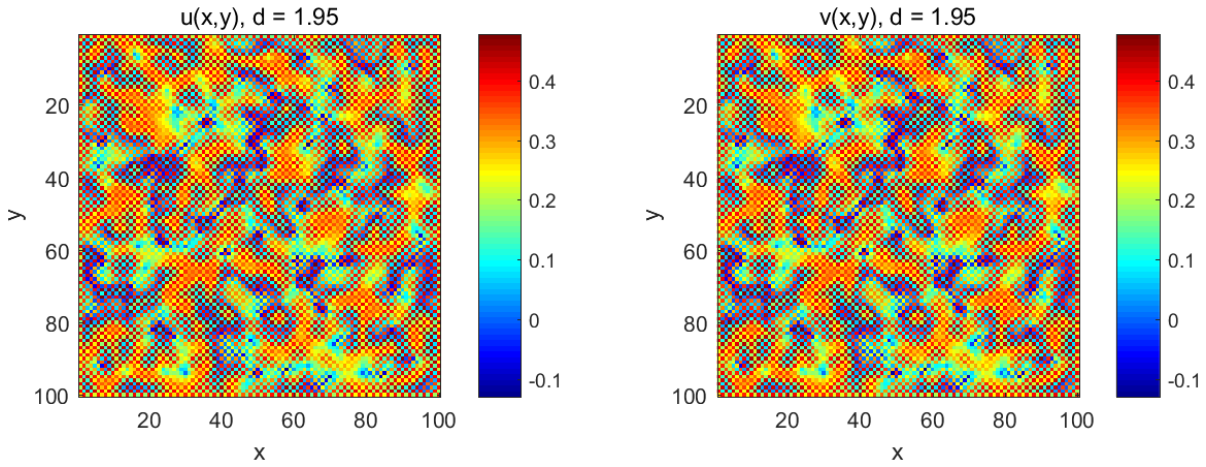

Fig.21. N=100, d=1.95, after 200,000 iterations (Neumann boundary conditions)

When d=1.95 and N=100, it can be seen from Figures 20 and 21 that after 10,000 iterations and 200,000 iterations, the patterns are both rich in color, and no obvious straight line segments are observed in the patterns.

V. CONCLUSION

In this paper, we discuss the Turing instability of the reaction–diffusion system (5) on graphs and present a linear mode decomposition of system (5). In Section 3, we consider the competitive Lotka–Volterra system. By choosing parameters $r_1 = r_2 = 2$, $a_1 = a_2 = 0.5$, we compute its positive fixed point and find the roots of the characteristic equation, and further obtain the condition for Turing instability. In Section 4, we select an N×N regular grid graph with 4-neighbor connectivity, considering both periodic and Neumann boundary conditions. Numerical simulations of system (15) are carried out on these graphs, and a rich variety of patterns are obtained.

In Section 4, we can see that for the same N and d, the patterns obtained from simulations are quite different under different boundary conditions. When d=1.28, for both N=10 and N=100, and under both boundary conditions, we observed periodic orbits. When d=1.95, the system eventually entered a chaotic state in all cases.

For future work, we can construct bifurcation diagrams and Lyapunov exponent diagrams to further analyze the conditions under which the system enters periodic orbits or a chaotic state.

ACKNOWLEDGMENTS

This work was financially supported by the 2024 Annual University-Level Scientific Research Project of Zhujiang College, South China Agricultural University (Grant No.2024ZJKYC004), and the 2025 Annual University-Level Scientific Research Project of Zhujiang College, South China Agricultural University (Grant No.2025KYXM019).

REFERENCES

[1]. Turing, A.M. The chemical basis of morphogenesis. Philosophical Transactions of the Royal Society of London. Series B, Biological Sciences, 237(641), 37–72 (1952) .

[2]. Nakao, H., & Mikhailov, A.S. Turing patterns in network-organized activator–inhibitor systems. Nature Physics, 6(7), 544–550 (2010).

[3]. Rodrigues, F.A., Peron, T.K.D., Ji, P., & Kurths, J.The Kuramoto model in complex networks. Physics Reports, 610, 1 – 98 (2016).

[4]. Pastor-Satorras, R., Castellano, C., Van Mieghem, P., & Vespignani, A. Epidemic processes in complex networks. Reviews of Modern Physics, 87(3), 925 – 979 (2015) .
[5]. Murray, J.D. Mathematical Biology (3rd ed.). Springer-Verlag (2002) .
[6]. Royle GF, Godsil C. Algebraic graph theory. New York: Springer (2001) .
[7]. Han YT, Han B, Zhang L, Xu L, Li MF, Zhang G. Turing instability and wave patterns for a symmetric discrete competitive Lotka-Volterra system. Wseas Trans Math; 10(5):181C9 (2011) .
[8]. Newman, M. W. , Libraty, N. , On, O. , On, K. A. , & On, K. A. . The Laplacian spectrum of graphs. graph theory, combinations and applications, 18(7), 871--898 (1991).